

Fermiophobic Higgs boson and supersymmetry

E. Gabrielli^{a,b}, K. Kannike^{a,c}, B. Mele^d, A. Racioppi^a, M. Raidal^{a,e,f}

(a) NICPB, Ravalja 10, Tallinn 10143, Estonia

(b) INFN, Sezione di Trieste, c/o Dipartimento di Fisica, Università di Trieste,
Via Valerio 2, I - 34127 Trieste, Italy

(c) Scuola Normale Superiore and INFN, Piazza dei Cavalieri 7, 56126 Pisa, Italy

(d) INFN, Sezione di Roma, c/o Dipartimento di Fisica, Università di Roma La Sapienza,
Piazzale A. Moro 2, I-00185 Rome, Italy

(e) Institute of Physics, University of Tartu, Estonia

(f) CERN, Theory Division, CH-1211 Geneva 23, Switzerland

ABSTRACT

If a light Higgs boson with mass 125 GeV is fermiophobic, or partially fermiophobic, then the MSSM is excluded. The minimal supersymmetric fermiophobic Higgs scenario can naturally be formulated in the context of the NMSSM that admits Z_3 discrete symmetries. In the fermiophobic NMSSM, the SUSY naturalness criteria are relaxed by a factor $N_c y_t^4/g^4 \sim 25$, removing the little hierarchy problem and allowing sparticle masses to be naturally of order 2–3 TeV. This scale motivates wino or higgsino dark matter. The SUSY flavour and CP problems as well as the constraints on sparticle and Higgs boson masses from $b \rightarrow s\gamma$, $B_s \rightarrow \mu\mu$ and direct LHC searches are relaxed in fermiophobic NMSSM. The price to pay is that a new, yet unknown, mechanism must be introduced to generate fermion masses. We show that in the fermiophobic NMSSM the radiative Higgs boson branchings to $\gamma\gamma$, γZ can be modified compared to the fermiophobic and ordinary standard model predictions, and fit present collider data better. Suppression of dark matter scattering off nuclei explains the absence of signal in XENON100.

March 2012

1 Introduction and motivation

The TeVatron [1, 2] and LHC experiments presented their new and updated results [3, 4, 5, 6, 7, 8, 9, 10, 11, 12] on searches for the Higgs boson [13] at the Moriond 2012 conference [14]. While on average the data is consistent with the standard model (SM) Higgs boson with mass 125 GeV, interesting anomalies start to emerge that may signal unexpected new physics in the Higgs sector. The most interesting of them is a local 3σ level excess in searches for the fermiophobic (FP) Higgs boson [15] in $\gamma\gamma$ final states both in the ATLAS and CMS experiments [16]. This signals that there is an anomalously large contribution in the observed $\gamma\gamma$ excess coming from the vector-boson fusion (VFB) Higgs production mechanism. Indeed, the relative weight of the latter and the associate production with W, Z (VH) is enhanced with respect to the SM dominant gluon-gluon fusion channel (ggF) in the FP high- p_T selections applied by the CMS and ATLAS. This anomaly is accompanied by a deficit of WW^* compared with the SM in all experiments.

The Higgs boson mass $M_h \approx 125$ GeV is peculiar in several ways. In the context of FP Higgs boson, there is an accident that at the 7–8 TeV LHC the Higgs boson signal rate in the $\gamma\gamma$ channel, $\sigma \times BR$, happens to be equal to the SM one in the vicinity of this Higgs mass value [17]. This is the reason why the LHC inclusive $\gamma\gamma$ excess is consistent with the FP Higgs boson. At the same time, the signal rates for other gauge boson channels, $WW^*, ZZ^*, Z\gamma$, are predicted to be 40–50% suppressed compared to the SM [17]. The $M_h \approx 125$ GeV Higgs boson is peculiar also because, for a SM-like Higgs of that mass, branching fractions for many decay channels are measurable at the LHC. Therefore, the LHC is, in principle, able to determine the nature and properties of the 125 GeV Higgs boson.

Motivated by these results we performed a global fit to all available collider data to determine which Higgs boson scenario is currently favoured [18], improving and extending similar pre-Moriond fits [19]. A purely FP Higgs boson gives a fit to present data almost as good as the SM one, but with very different predictions for the signal rates at the LHC. A partially FP Higgs boson, however, gives a significantly better fit to current data than the SM [18]. This is because the FP Higgs qualitatively describes the observed anomalies in the data correctly, although it predicts larger signal rates than observed. Small additional branching fractions into fermionic channels, for example into $b\bar{b}$, decrease the overall rate and improve the fit to data significantly.

Partial fermiophobia is exactly what is expected to happen when considering the FP Higgs boson scenario as an effective low energy theory in the context of quantum field theory [20]. Because the SM fermions are massive, at loop level non-vanishing Yukawa couplings are generated even if at some high new physics scale the Higgs boson was initially purely fermiophobic. As long as the fermion mass generating mechanism is unknown, the induced Yukawa couplings represent an uncertainty in the low energy FP Higgs model. Present data suggest that the Higgs boson might be partially fermiophobic [17, 20, 21].

The 125 GeV Higgs boson is also unsatisfactory, because this mass is below the SM vacuum stability bound in case new physics appears only above the scale of gauge coupling unifica-

tion [22]. The vacuum stability can be made consistent with the 125 GeV Higgs mass [23] by extending the scalar sector with dark matter candidates [24, 25]. But the simplest solution is provided by (partial) fermophobia. Because the vacuum instability is caused by the large top Yukawa coupling in the SM, reducing its value makes the hinted Higgs mass compatible with the GUT scale.

It is well known that the existence of the Higgs boson rises a question of why the electroweak scale is so much smaller than the Planck scale. The most elegant solution to that problem is given by supersymmetry (SUSY). However, direct and indirect collider bounds, cosmological dark matter abundance and constraints from dark matter direct detection experiments together with a Higgs boson mass of 125 GeV impose stringent constraints on SUSY scale in most popular SUSY models – the MSSM [26, 27] and NMSSM [28, 29]. The constraint $M_{\text{SUSY}} > 1 \text{ TeV} \gg M_Z$ reintroduces severe fine tuning to theory, known as the little hierarchy problem [30], that makes SUSY as a solution to the hierarchy problem unnatural.

If the Higgs boson turns out to be fermiophobic, some SUSY models are in even more serious trouble. We show that fermiophobia and a Higgs boson mass at 125 GeV together exclude all versions of the MSSM independently of any model detail. This is because in the MSSM the upper bound on the tree level Higgs boson mass is M_Z , and large radiative corrections, dominated by stop contributions, are needed to reach 125 GeV. Fermiophobia removes the dominant stop loops as they are induced by Yukawa couplings. There might be large trilinear scalar couplings, the A -terms, but their contribution to M_h^2 is negative. Dimensionful trilinear couplings may trigger electroweak symmetry breaking [31] via a dimensionful Coleman-Weinberg [32] mechanism, but cannot increase the Higgs boson mass.

Nevertheless, SUSY models with additional tree level contributions to the Higgs boson mass, such as the NMSSM, are viable fermiophobic SUSY theory candidates. In fact fermiophobia can cure some SUSY problems and make it more compatible with experimental data. Firstly, the fine tuning problem of SUSY, also coming from loop contributions to the Higgs boson mass squared, is now induced by gauge couplings, improving the fine tuning by a factor of $N_c y_t^4/g^4 \sim 25$. This improvement completely removes the little hierarchy problem. SUSY masses of order 2-3 TeV become completely natural. Allowing for some fine tuning, even the split SUSY [33] with a very heavy scalar sector becomes viable. This would explain why no sparticles have been discovered by the LHC up to now [34, 35]. Secondly, SUSY flavour and CP problems are improved by removing (or decreasing) the Yukawa couplings and by allowing also squark and slepton masses to be at a few-TeV scale. Thirdly, the additional Higgs bosons can be light. For example, the absence of constraints from $b \rightarrow s\gamma$ and $B_s \rightarrow \mu\mu$ [36] allows the charged Higgs boson to be light, opening again the possibility for its discovery at the LHC. Fourthly, the SUSY fermion sector may be either light or heavy. While gluinos could have been abundantly produced at the LHC if they were very light, for colourless fermions there would exist only collider bounds from LEP and Tevatron. Fifthly, the constraints on dark matter are relaxed. Because neutralino elastic scattering off nuclei is dominated by tree level Higgs boson exchange, this process would be suppressed and the prospects for dark matter discovery at the XENON100 are decreased in this scenario [37]. As the SUSY scale could now be large, higgsino or wino relic abundance would become a natural explanation to the dark matter of

the Universe.

The obvious question in any FP Higgs boson scenario is what is the alternative mechanism for generating the observed fermion masses. Because the top quark mass is so large, it cannot be generated radiatively. The most plausible scenario for generating such large fermion masses is strong dynamics above the electroweak scale [38]. In such a scenario both the composite Higgs boson fermiophobia and fermion masses might originate from the same new physics. A generic prediction of strong electroweak symmetry breaking scenarios, including composite Higgs models, is the appearance of new resonances at 2–3 TeV. In the following, we assume that such or any other new physics scenario above the electroweak scale generates the top quark mass.

In this work we formulate a FP NMSSM as a minimal FP SUSY model. Originally the NMSSM was constructed to solve the μ problem of the MSSM and to have an additional contribution to the masses of the Higgs bosons. To achieve that, an additional Z_3 symmetry is usually imposed on the NMSSM. We show that choosing quantum numbers of this symmetry appropriately, superpotential Yukawa terms may be forbidden in the NMSSM. In this case, all the pros and contras of FP SUSY discussed above apply also to the FP NMSSM. In our phenomenological study of the model we concentrate on radiatively induced Higgs boson decays $h \rightarrow \gamma\gamma$ and $h \rightarrow Z\gamma$. This choice is motivated by the fact that SUSY effects most easily show up in loop level processes. Our aim is to study whether the FP SUSY Higgs boson gives a better or worse phenomenological fit to the LHC data than the FP SM Higgs boson. We find that the new SUSY contribution can enhance or reduce the $\gamma\gamma$ and $Z\gamma$ rates as much as 50% compared to the FP SM Higgs depending on the sign of the μ parameter. Because the data prefers smaller rates [18], the FP SUSY Higgs can give a better fit to data than the SM.

We note that in the MSSM the WW^* and ZZ^* rates can be reduced at tree level compared to the SM. At the same time, the decay $h \rightarrow \gamma\gamma$ is dominated by the W -boson loop, introducing a correlation between the two processes. Should the observed deficit in WW^* persist together with the $\gamma\gamma$ excess, new physics beyond the MSSM would be required. A FP NMSSM might be a good candidate for such new physics.

The paper is organized as follows. In section 2 we study fermiophobic Higgs scenarios in SUSY. In section 3 we study the radiative decays $h \rightarrow \gamma\gamma$ and $h \rightarrow Z\gamma$ in a specific parameter region of the FP NMSSM model. In section 4 we add some discussion and conclude in section 5.

2 Fermiophobic supersymmetry

To formulate a supersymmetric FP Higgs boson theory, the first attempt should be made in the MSSM. However, we are going to show that the Higgs boson mass $M_h \approx 125$ GeV is by far too large to be generated in the FP MSSM since loop corrections from the top Yukawa coupling are absent. The dominant SUSY loop contribution to the Higgs mass in the FP MSSM comes from the large trilinear A -term, but this contribution is always negative. Thus the FP MSSM is definitely excluded on phenomenological grounds. In order to rescue supersymmetry, we show

that the NMSSM offers a natural framework to formulate a supersymmetric FP Higgs scenario consistent with experimental results.

2.1 Fermiophobic MSSM

The well known MSSM superpotential is

$$\mathcal{W} = y_u Q H_u u^c + y_d H_d Q d^c + y_e H_d L e^c + \mu H_u H_d, \quad (1)$$

where y_u , y_d and y_e are the up quark, down quark and charged lepton Yukawa couplings. The LHC hints for a FP Higgs imply that at least the third generation Yukawa couplings must be strongly suppressed compared to their SM values so that the production mechanism $gg \rightarrow h$ and the decay channels $h \rightarrow b\bar{b}$, $h \rightarrow \tau\bar{\tau}$ become subdominant compared to the gauge boson processes. Following this indication, in this paper we study its implications without trying to explain the suppression of Yukawa couplings in the context of MSSM. Thus, for simplicity, we just take $y_u = y_d = y_e = 0$.

In the MSSM the tree level Higgs boson mass has the well known upper bound $M_h^{\text{tree}} < M_Z$. This comes from the fact that in SUSY the Higgs quartic couplings are generated by gauge couplings via the D -terms. As the Higgs boson quartic coupling is the only free parameter in the SM Higgs sector, in the MSSM there is no freedom to tune the tree level Higgs boson mass. To be consistent with experimental data, in the MSSM very large positive loop corrections to M_h^2 must be generated. Those loop corrections are dominated by top squark contributions that are induced by the top Yukawa coupling y_t [39],

$$\Delta M_h^2 = 3y_t^4 \frac{v^2 \sin^4 \beta}{8\pi^2} \left[\log \frac{M_S^2}{m_t^2} + \frac{X_t^2}{M_S^2} \left(1 - \frac{X_t^2}{12M_S^2} \right) \right], \quad (2)$$

where M_S is the average stop mass, $\tan \beta = v_u/v_d$, $v^2 = v_u^2 + v_d^2$, and X_t is the stop mass mixing parameter

$$X_t = A_t - \mu \cot \beta = \frac{a_t}{y_t} - \mu \cot \beta, \quad (3)$$

where a_t is the trilinear coupling of the soft term $a_t \tilde{Q} H_u \tilde{u}^c$. In order to achieve the Higgs boson mass indicated by the LHC experiments, $M_h \approx 125$ GeV, Eq. (2) implies that the stop masses must exceed TeV scale.

In the FP MSSM the dominant stop contribution is absent since we take $y_t \rightarrow 0$. However, loops induced by very large trilinear soft interaction $a_t \tilde{Q} H_u \tilde{u}^c$ with $a_t > 1$ TeV are still allowed in general MSSM even in the absence of Yukawa couplings. In the FP limit we obtain

$$\Delta M_h^2 = -\frac{3v^2 \sin^4 \beta}{8\pi^2} \frac{a_t^4}{12M_S^4}, \quad (4)$$

that is negative. The dimensionful couplings like the A -terms may be used to generate negative Higgs mass terms radiatively, thus generating dynamical breaking of electroweak symmetry [31],

but they do not increase the Higgs mass prediction in the MSSM. This is because the Higgs boson quartic self coupling is fixed by the D -term that gives the upper bound. As the chargino loop contributions to the Higgs boson mass are of order few GeV, in the FP MSSM the Higgs boson mass 125 GeV is not achievable. Independently of model details, the FP MSSM is excluded by the Higgs boson mass.

2.2 Fermiophobic NMSSM

NMSSM is the next to minimal supersymmetric standard model whose particle content is extended by a gauge singlet chiral superfield S (for reviews and references therein see [28]). The original motivation for the NMSSM was to explain why the MSSM superpotential parameter $\mu H_u H_d$ is of the same order as the soft SUSY breaking parameters. In addition, in the NMSSM the Higgs bosons obtain tree level mass not determined by the D -terms, thus allowing larger Higgs masses than M_Z . To achieve those goals, usually the most general NMSSM is constrained by imposing an additional Z_3 symmetry in addition to the R -parity. Those properties make the NMSSM our prime candidate for the minimal FP SUSY model. The superpotential of the FP NMSSM that we would like to obtain is given by

$$\mathcal{W} = \lambda S H_u H_d + \frac{\kappa}{3} S^3, \quad (5)$$

together with the following soft SUSY breaking terms

$$\mathcal{L}_{\text{soft}} = - \left(m_{h_u}^2 h_u^\dagger h_u + m_{h_d}^2 h_d^\dagger h_d + m_s^2 s^\dagger s \right) - \left(a_\lambda s h_u h_d + \frac{1}{3} a_k s^3 + \text{h.c.} \right), \quad (6)$$

where s stands for the scalar component of the singlet chiral superfield S . Thus we have to forbid the $\mu H_u H_d$, S , S^2 , $y_u Q H_u u^c$, $y_d H_d Q d^c$, $y_e H_d L e^c$ terms by imposing an additional Z_N symmetry and appropriately choosing the Z_N charges to satisfy the following constraints

$$X_Q + X_{H_u} + X_{u^c} \neq 0 \pmod{N}, \quad (7)$$

$$X_Q + X_{H_d} + X_{d^c} \neq 0 \pmod{N}, \quad (8)$$

$$X_L + X_{H_d} + X_{e^c} \neq 0 \pmod{N}, \quad (9)$$

$$X_{H_u} + X_{H_d} \neq 0 \pmod{N}, \quad (10)$$

$$X_S \neq 0 \pmod{N}, \quad (11)$$

$$2X_S \neq 0 \pmod{N}, \quad (12)$$

$$3X_S = 0 \pmod{N}, \quad (13)$$

$$X_S + X_{H_u} + X_{H_d} = 0 \pmod{N}. \quad (14)$$

One could choose $X_L = X_Q$ and $X_{e^c} = X_{d^c}$, then (9) would be superfluous.

For Z_3 , if $X_{H_u} = X_{H_d} = X_S = 1$ and $X_{\text{fermion}} = 0$, the above equations are satisfied. In addition, the lowest order Yukawa couplings can be generated via $d = 6$ operator $\frac{\langle H_d^\dagger \rangle \langle H_d \rangle}{\Lambda^2} Q H_d d^c$, where Λ is the scale of new physics. This demonstrates that small but non-vanishing Yukawa couplings

should exist also in the FP Higgs scenarios. On the other hand, if $X_{H_u} = X_{H_d} = X_S = 1$ and $X_{\text{fermion}} = 2$, the above equations are also satisfied, but the lowest order Yukawas would be generated as e.g. $\frac{\langle S \rangle}{\Lambda} Q H_d d^c$. These charges satisfy two additional equations

$$X_Q + X_{H_u} + X_{u^c} + X_S = 0, \quad (15)$$

$$X_Q + X_{H_d} + X_{d^c} + X_S = 0. \quad (16)$$

This could possibly generate the Yukawa couplings for the first two generations but not for the top quark. Therefore we have to assume that the significant amount of third generation fermion masses should come from some additional mechanism. The prime candidate for such a mechanism is some strong dynamics above 2–3 TeV scale.

The Z_3 symmetry could come from the breaking of an $U(1)'$ [40]. In this case one has to keep in mind the possibility of discrete gauge anomalies [41]. In the NMSSM these have been considered in [42]. If one chooses $X_{\text{fermion}} = 0$, the anomaly constraints can be simply evaded.

Breaking of the Z_3 symmetry in the early universe could create a problem with the domain walls that produce an anisotropy in the CMB and ruin nucleosynthesis [43]. The problem can be solved by allowing for radiative generation of small renormalisable Z_3 breaking terms [44].

3 Phenomenology of FP NMSSM Higgs bosons at the LHC

Our aim in this section is to study radiatively induced decays $h \rightarrow \gamma\gamma$ and $h \rightarrow Z\gamma$ of the SM-like FP Higgs boson in the context of NMSSM. If there are light superparticles or light additional Higgs bosons, their effects are first expected to show up in loop level processes. However, before proceeding with this study, we have to show that the FP NMSSM is a viable model. Therefore we start studying the FP NMSSM Higgs sector. We do not attempt to scan the full parameter space of the model. Instead, we start by fixing the parameters in the Higgs sector to one particularly interesting point with $\tan\beta = 1$ and decoupled CP-even singlet, that allows for two following Higgs scenarios: (*i*) the 125 GeV excess is due to the lightest CP-even Higgs boson, the remaining neutral Higgs bosons are too heavy and have no direct decays to two gauge bosons; (*ii*) the 125 GeV excess is due to the next-to-lightest CP-even Higgs boson, the lightest one has no direct decays into two gauge bosons and remains invisible at the LHC. Here, we will focus on scenario (*i*). Then, we relax the condition $\tan\beta = 1$ and analyze the impact of a $\tan\beta \neq 1$ value, in the approximation in which the scalar singlet is very heavy. We finally show how the FP NMSSM can be distinguished from the FP SM by studying the radiatively induced Higgs boson decays.

3.1 Scalar potential and masses

The FP NMSSM scalar potential derived from Eq. (5), Eq. (6) and also from the D -term contributions is

$$\begin{aligned} V = & \left(m_{h_u}^2 + |\lambda s|^2 \right) \left(|h_u^0|^2 + |h_u^+|^2 \right) + \left(m_{h_d}^2 + |\lambda s|^2 \right) \left(|h_d^0|^2 + |h_d^-|^2 \right) \\ & + m_s^2 |s|^2 + \left(a_\lambda (h_u^+ h_d^- - h_u^0 h_d^0) s + \frac{1}{3} a_k s^3 + \text{h.c.} \right) \\ & + |\lambda (h_u^+ h_d^- - h_u^0 h_d^0) + k s^2|^2 \\ & + \frac{g_1^2 + g_2^2}{8} \left(|h_u^0|^2 + |h_u^+|^2 - |h_d^0|^2 - |h_d^-|^2 \right)^2 + \frac{g_2^2}{2} |h_u^+ h_d^{0*} + h_u^0 h_d^{-*}|^2. \end{aligned} \quad (17)$$

We suppose for simplicity that all the parameters in Eq. (17) are real. We have checked that the potential is always bounded from below. Supposing that only the real parts of Higgs bosons can get vacuum expectation values (VEVs) different from zero and parametrizing the fields as

$$h_d^0 = \frac{1}{\sqrt{2}} (v_d + h_{dR}^0 + i h_{dI}^0), \quad h_u^0 = \frac{1}{\sqrt{2}} (v_u + h_{uR}^0 + i h_{uI}^0), \quad s = \frac{1}{\sqrt{2}} (v_S + s_R + i s_I), \quad (18)$$

we get the following equations for the stationary points

$$\begin{aligned} v \left(-4v_S \sin \beta \left(\sqrt{2}a_\lambda + k\lambda^2 v_S \right) + \cos \beta \left(-v^2 \sin^2 \beta (g_1^2 + g_2^2 - 4\lambda^2) + 8m_{h_d}^2 + 4\lambda^2 v_S^2 \right) \right. \\ \left. + v^2 \cos^3 \beta (g_1^2 + g_2^2) \right) = 0, \end{aligned} \quad (19)$$

$$\begin{aligned} v \left(-4v_S \cos \beta \left(\sqrt{2}a_\lambda + k\lambda^2 v_S \right) + \sin \beta \left(v^2 \sin^2 \beta (g_1^2 + g_2^2) + 8m_{h_u}^2 + 4\lambda^2 v_S^2 \right) \right. \\ \left. - v^2 \sin \beta \cos^2 \beta (g_1^2 + g_2^2 - 4\lambda^2) \right) = 0, \end{aligned} \quad (20)$$

$$v_S \left(\sqrt{2}a_k v_S + \lambda^2 (2k^2 v_S^2 + v^2) + 2m_S^2 \right) - \frac{1}{4} v^2 \sin(2\beta) \left(\sqrt{2}a_\lambda + 2k\lambda^2 v_S \right) = 0. \quad (21)$$

First of all we must avoid that $v_u = v_d = v_S = 0$ is a minimum of the potential. This can be done by requiring

$$m_{h_u}^2 m_{h_d}^2 m_s^2 < 0. \quad (22)$$

Now let us give a look at the Hessian matrix in the minimum. In the basis $(h_{dR}^0, h_{uR}^0, s_R)$ we have for the CP-even Higgs bosons

$$M_S^2 = \begin{pmatrix} M_{S,11}^2 & M_{S,12}^2 & M_{S,13}^2 \\ \dots & M_{S,22}^2 & M_{S,23}^2 \\ \dots & \dots & M_{S,33}^2 \end{pmatrix}, \quad (23)$$

where

$$M_{S,11}^2 = m_{h_d}^2 + \frac{v_S^2 \lambda^2}{2} + \frac{1}{8} v^2 (g_1^2 + g_2^2 + 2\lambda^2 + 2(g_1^2 + g_2^2 - \lambda^2) \cos(2\beta)), \quad (24)$$

$$M_{S,22}^2 = m_{h_u}^2 + \frac{v_S^2 \lambda^2}{2} + \frac{1}{8} v^2 (g_1^2 + g_2^2 + 2\lambda^2 - 2(g_1^2 + g_2^2 - \lambda^2) \cos(2\beta)), \quad (25)$$

$$M_{S,33}^2 = m_S^2 + 3k^2 v_S^2 + \sqrt{2} a_k v_S + v^2 \left(\frac{\lambda^2}{2} - k\lambda^2 \cos \beta \sin \beta \right), \quad (26)$$

$$M_{S,12}^2 = \frac{1}{8} (-g_1^2 - g_2^2 + 4\lambda^2) \sin(2\beta) v^2 - \frac{1}{2} k v_S^2 \lambda - \frac{a_\lambda v_S}{\sqrt{2}}, \quad (27)$$

$$M_{S,13}^2 = v v_S (\lambda^2 \cos \beta - k \lambda \sin \beta) - \frac{a_\lambda v \sin \beta}{\sqrt{2}}, \quad (28)$$

$$M_{S,23}^2 = v v_S (\lambda^2 \sin \beta - k \lambda \cos \beta) - \frac{a_\lambda v \cos \beta}{\sqrt{2}}. \quad (29)$$

So far the results have been general. However, we can see from the mass matrix that there is a choice of the parameters that allows no mixing between s and $h_{u,d}^0$,

$$\tan \beta = 1, \quad (30)$$

$$k = \lambda, \quad (31)$$

$$a_\lambda = 0. \quad (32)$$

Notice that $\tan \beta = 1$ is allowed in this model because no constraints occur from the scalar potential minimization nor from the Yukawa sector. Therefore this choice is the most natural one. Adopting, for simplicity, the choice in eqs. (30)-(32) and requiring, of course, $v_u \neq 0, v_d \neq 0, v_S \neq 0$, the minimization equations read

$$(4m_{h_d}^2 + \lambda^2 v^2) = 0, \quad (33)$$

$$(4m_{h_u}^2 + \lambda^2 v^2) = 0, \quad (34)$$

$$\frac{a_k v_S^2}{\sqrt{2}} + m_S^2 v_S + \lambda^2 v_S^3 = 0, \quad (35)$$

leading to the CP-even neutral Higgs boson mass matrix

$$M_S^2 = \begin{pmatrix} \frac{1}{2} (M_Z^2 + v_S^2 \lambda^2) & \frac{1}{2} ((v - v_S)(v + v_S)\lambda^2 - M_Z^2) & 0 \\ \frac{1}{2} ((v - v_S)(v + v_S)\lambda^2 - M_Z^2) & \frac{1}{2} (M_Z^2 + v_S^2 \lambda^2) & 0 \\ 0 & 0 & 2v_S^2 \lambda^2 + \frac{a_k v_S}{\sqrt{2}} \end{pmatrix}, \quad (36)$$

where $M_Z^2 = \frac{1}{4} (g_1^2 + g_2^2) v^2$. The corresponding eigenvalues

$$M_{h_1^0}^2 = \frac{\lambda^2 v^2}{2}, \quad (37)$$

$$M_{h_2^0}^2 = M_Z^2 + \frac{1}{2} \lambda^2 (2v_S^2 - v^2), \quad (38)$$

$$M_{s_R}^2 = \frac{a_k v_S}{\sqrt{2}} + 2\lambda^2 v_S^2, \quad (39)$$

correspond to the eigenvectors

$$h_1^0 = \frac{1}{\sqrt{2}} (h_{dR}^0 + h_{uR}^0), \quad (40)$$

$$h_2^0 = \frac{1}{\sqrt{2}} (h_{dR}^0 - h_{uR}^0). \quad (41)$$

Two distinct phenomenologically viable scenarios occur. Since we would like to identify one of the CP-even eigenstates with the 125 GeV resonance hinted at by the LHC, it has to be made of doublets. If $M_{h_1^0}^2 < M_{h_2^0}^2$ then, in the notation of the MSSM, $h = h_1^0$, $H = h_2^0$, and the Higgs mixing angle is given by $\alpha = -\pi/4 = \beta - \pi/2$. In that case H does not have any direct tree level coupling to WW and ZZ that explains why the LHC does not see presently any other resonance, but the lightest one at 125 GeV. On the other hand, if $M_{h_1^0}^2 > M_{h_2^0}^2$ then $h = h_2^0$, $H = h_1^0$, and the Higgs mixing angle is $\alpha = \pi/4 = \beta$. In this case the LHC observed the second heaviest CP-even state because the couplings of the lightest one to fermions and to gauge bosons are strongly suppressed. Discovering such a light “sterile” Higgs boson is very difficult at the LHC.

The CP-odd Higgs boson mass matrix in the basis $(h_{dI}^0, h_{uI}^0, s_I)$ is given by

$$M'^2_P = \begin{pmatrix} \frac{v_S^2 \lambda^2}{2} & \frac{v_S^2 \lambda^2}{2} & -\frac{vv_S \lambda^2}{\sqrt{2}} \\ \frac{v_S^2 \lambda^2}{2} & \frac{v_S^2 \lambda^2}{2} & -\frac{vv_S \lambda^2}{\sqrt{2}} \\ -\frac{vv_S \lambda^2}{\sqrt{2}} & -\frac{vv_S \lambda^2}{\sqrt{2}} & v^2 \lambda^2 - \frac{3a_k v_S}{\sqrt{2}} \end{pmatrix}, \quad (42)$$

and the corresponding eigenvalues are

$$M_{G^0}^2 = 0, \quad (43)$$

$$M_{A_1^0}^2 = \frac{1}{4} \left(2\lambda^2 (v^2 + v_S^2) - 3\sqrt{2}a_k v_S - \sqrt{\left(3\sqrt{2}a_k v_S - 2\lambda^2 (v^2 + v_S^2) \right)^2 + 24\sqrt{2}a_k \lambda^2 v_S^3} \right) \quad (44)$$

$$M_{A_2^0}^2 = \frac{1}{4} \left(2\lambda^2 (v^2 + v_S^2) - 3\sqrt{2}a_k v_S + \sqrt{\left(3\sqrt{2}a_k v_S - 2\lambda^2 (v^2 + v_S^2) \right)^2 + 24\sqrt{2}a_k \lambda^2 v_S^3} \right) \quad (45)$$

While in (36) we cancelled the singlet-doublet mixing in the CP-even sector by a particular choice of parameters, such a mixing still occurs in the CP-odd sector.

Finally the charged Higgs mass matrix in the basis $(h_u^+, h_d^{-*} = h_d^+)$ is given by

$$M'^2_\pm = \left(M_W^2 + \frac{1}{2}\lambda^2 (2v_S^2 - v^2) \right) \begin{pmatrix} 1 & 1 \\ 1 & 1 \end{pmatrix}, \quad (46)$$

where $M_W^2 = \frac{1}{4}g_2^2 v^2$. It contains one massless Goldstone mode, and one massive eigenstate

$$M_{H^\pm}^2 = M_W^2 + \frac{1}{2}\lambda^2 (2v_S^2 - v^2), \quad (47)$$

$$H^\pm = \frac{1}{\sqrt{2}} (h_u^+ + h_d^{-*}). \quad (48)$$

The charged Higgs sector is identical to the MSSM one because S is electrically neutral. The matching can be easily done with the substitutions

$$\begin{aligned}\mu &\rightarrow \frac{1}{\sqrt{2}}\lambda v_S, \\ b &\rightarrow \frac{1}{2}v_S^2.\end{aligned}\tag{49}$$

Finally, we must ensure that all physical square masses are positive, which is equivalent to checking that our solution is a minimum of the potential. Moreover the constraint on $M_{H^\pm}^2$ implies that we are not breaking the $U(1)_{\text{em}}$. Up to now we only prevented the origin to be a minimum solution. So such a requirement will impose further constraints on the free parameters, that can be summarized as follows:

$$\text{sign}(a_k) = -\text{sign}(v_S), \quad |a_k| < 2\sqrt{2}\lambda^2|v_S|,\tag{50}$$

and one of the two following options

- a) $v_S^2 > \frac{1}{2}v^2$,
- b) $\frac{1}{2}\lambda^2(v^2 - 2v_S^2) < M_W^2$.

From now on we shall assume that the lightest CP even scalar is the one coupled to the W 's, thus $M_{h_1^0}^2 < M_{h_2^0}^2$. Moreover we want also $M_{h_1^0}^2 > M_Z^2$. This implies that the only available option is a). This fixes also the lightest CP-even Higgs couplings to gauge bosons to be exactly as in the SM. The lightest CP-even Higgs couples to the charged Higgs with

$$\lambda_{hH^+H^-} = 2c_W^2 - \frac{\lambda^2}{2} \frac{v^2}{M_Z^2},\tag{51}$$

where in our notation $c_W = \cos \theta_W$, $s_W = \sin \theta_W$ with θ_W the Weinberg angle, and the coupling is normalized according to the conventions in [26]. The first term is the MSSM contribution for $\alpha = -\pi/4 = \beta - \pi/2$, while the term in λ is the NMSSM correction.

We now consider the impact of relaxing the $\tan \beta = 1$ condition in the present analysis. We assume as usual that the scalar singlet is very heavy, and $kv_S \gg M_Z, a_k, a_\lambda$. Within such approximation it is easy to derive [28] that $\alpha \simeq \beta - \pi/2$ still holds, and H is again essentially decoupled from WW or ZZ . On the other hand, one has

$$M_h^2 \simeq M_Z^2 \cos^2(2\beta) + \frac{1}{2}\lambda^2 v^2 \sin^2(2\beta) - \frac{\lambda^2}{k^2} v^2 (\lambda - k \sin(2\beta))^2.\tag{52}$$

Hence, the presence of the singlet can still give a negative contribution to the light Higgs boson mass. To prevent the latter negative contribution, we generalize eq. (31), and assume

$$k = \lambda / \sin(2\beta)\tag{53}$$

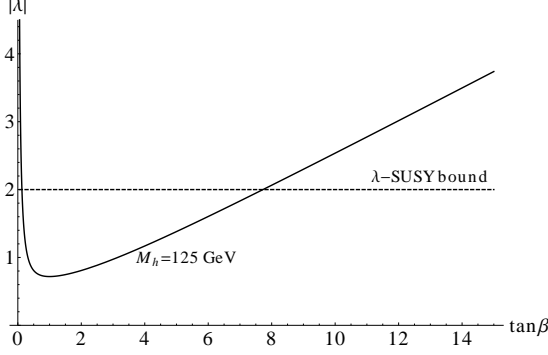


Figure 1: . Contour of $M_h = 125$ GeV in the $(\tan \beta, |\lambda|)$ plane (solid line). The dashed line is the λ -SUSY upper bound.

so that

$$M_h^2 \simeq M_Z^2 \cos^2(2\beta) + \frac{1}{2} \lambda^2 v^2 \sin^2(2\beta). \quad (54)$$

Here, we are interested in values of λ and $\tan \beta$ that satisfy $M_h \approx 125$ GeV. In Fig. 1 we plot the corresponding two-dimentional curve of $|\lambda|$ versus $\tan \beta$. The black continuous line represents $M_h = 125$ GeV. In the λ -SUSY theory [45], λ is increased so that the interaction becomes non-perturbative below the unification scale. However, λ should not exceed ~ 2 , otherwise non-perturbative physics would appear below 10 TeV, spoiling our understanding of precision electroweak data in the perturbative theory. The dashed line in Fig. 1 represents the λ -SUSY upper bound. Then, only low values of $\tan \beta$ are allowed, in the range $\tan \beta < 8$. In particular, $\tan \beta = 1$ corresponds to the minimal λ value ($\lambda \simeq 0.72$).

Finally, the relevant quantities for the charged Higgs phenomenology in the general $\tan \beta$ case are

$$M_{H^\pm}^2 = \frac{\lambda^2 v_S^2}{\sin^2(2\beta)} + M_W^2 - \frac{\lambda^2 v^2}{2} \quad (55)$$

$$\lambda_{hH^+H^-} = \cos(2\beta) \sin(\alpha + \beta) + 2c_W^2 \sin(\beta - \alpha) - \frac{\lambda^2}{2} \frac{v^2}{M_Z^2} \cos(\alpha + \beta) \sin(2\beta). \quad (56)$$

3.2 Neutralinos and charginos

The soft SUSY breaking gaugino mass terms in the Lagrangian read

$$\mathcal{L} = -\frac{1}{2} (M_1 \lambda_1 \lambda_1 + M_2 \lambda_2^i \lambda_2^i + M_3 \lambda_3^a \lambda_3^a). \quad (57)$$

In the basis $\psi^0 = (\lambda_1, \lambda_2^3, \tilde{h}_d^0, \tilde{h}_u^0, \tilde{s})$, the resulting mass terms in the Lagrangian read

$$\mathcal{L} = -\frac{1}{2} (\psi^0)^T \mathcal{M}_0 (\psi^0) + \text{h.c.} \quad (58)$$

where

$$M_0 = \begin{pmatrix} M_1 & 0 & -M_Z s_W \cos \beta & M_Z s_W \sin \beta & 0 \\ \dots & M_2 & M_Z c_W \cos \beta & -M_Z c_W \sin \beta & 0 \\ \dots & \dots & 0 & -\frac{1}{\sqrt{2}} \lambda v_S & -\frac{\lambda v}{\sqrt{2}} \sin \beta \\ \dots & \dots & \dots & 0 & -\frac{\lambda v}{\sqrt{2}} \cos \beta \\ \dots & \dots & \dots & \dots & \sqrt{2} k v_S \end{pmatrix}. \quad (59)$$

Because of supersymmetry and electric charge conservation the chargino sector is the same as the MSSM up to the substitutions (49), in the gauge-eigenstate basis $\psi^\pm = (\tilde{W}^+, \tilde{H}_u^+, \tilde{W}^-, \tilde{H}_d^-)$ the chargino mass terms in the Lagrangian are

$$\mathcal{L}_{\text{chargino mass}} = -\frac{1}{2}(\psi^\pm)^T \mathbf{M}_{\tilde{C}} \psi^\pm + h.c. \quad (60)$$

where, in 2×2 block form,

$$M_{\tilde{C}} = \begin{pmatrix} \mathbf{0} & \mathbf{X}^T \\ \mathbf{X} & \mathbf{0} \end{pmatrix}, \quad (61)$$

with

$$\mathbf{X} = \begin{pmatrix} M_2 & \sqrt{2} M_W \sin \beta \\ \sqrt{2} M_W \cos \beta & \frac{1}{\sqrt{2}} \lambda v_S \end{pmatrix}. \quad (62)$$

3.3 Radiative Higgs boson decays

The model we have chosen to work with leaves the FP Higgs boson decays to WW^* and ZZ^* final states at tree level unaffected compared to the FP SM predictions. Although it is easy in this framework to decrease the coupling at tree level by choosing a different $\tan \beta$ and the Higgs mixing parameter α , in the FP Higgs scenario this will also suppress the induced $\gamma\gamma$ rate because the latter is dominated by the W -boson loop. Because fermiophobia by itself is able to explain the observed deficit in WW^* channel [17], our choice is motivated by a maximized $\gamma\gamma$ rate. Therefore the deviations from the FP SM predictions may happen only due to extra particles in the loop. Because in the FP Higgs scenario the flavour physics constraints on charged Higgs masses are largely removed and chargino could be light, those particles can be as light as their present lower bounds from LEP II.

The free parameters at the EW scale which are relevant for our analysis are the following: $\tan \beta$, the gaugino masses M_1 and M_2 , the μ term given by $\mu \equiv \lambda v_S / \sqrt{2}$, the sign(μM_1) and sign(μM_2). In the present model, the mass of the charged Higgs is fixed once the value of μ is given, see Eq.(47). Moreover, we have chosen the convention of keeping M_2 positive, and allowing sign(μ) to vary. We have set $M_h = 125$ GeV, $M_1 = 100$ GeV and $\sqrt{s} = 7$ TeV.

Then, $\tan \beta$, $|\mu|$, sign(μ) and M_2 are free parameters. We chose to re-express $|\mu|$ and M_2 as functions of two physical mass parameters: the charged Higgs mass (M_{H^+}) and the lightest

chargino mass ($M_{\chi_L^+}$), as follows

$$|\mu| = \frac{\sqrt{M_h^2 + (M_{H^+}^2 - M_W^2) \sin^2(2\beta) - M_Z^2 \cos^2(2\beta)}}{\sqrt{2}} \quad (63)$$

$$M_2 = \frac{\pm \sqrt{2} M_{\chi_L^+} \sqrt{4 M_W^2 (\mu^2 - M_{\chi_L^+}^2) + 2 (M_{\chi_L^+}^2 - \mu^2)^2 + M_W^4 (1 - \cos 4\beta) - 2\mu M_W^2 \sin 2\beta}}{2(M_{\chi_L^+}^2 - \mu^2)}. \quad (64)$$

There are two different values of the gaugino mass M_2 , corresponding to the same lightest chargino mass. For convention $M_2 > 0$ and, for each sign(μ) and $|\mu|$ value, only one of the two solutions is allowed. Finally, we recall that the λ parameter is determined by M_h and β as

$$|\lambda| = \frac{\sqrt{2} \sqrt{M_h^2 - M_Z^2 \cos^2(2\beta)}}{v \sin(2\beta)}. \quad (65)$$

In Table 1, we give some numerical values of the input parameters and the corresponding derived fundamental parameters, for $M_h = 125$ GeV and $M_{H^+} = 400$ GeV.

| Input parameters | | | Derived parameters | | |
|------------------|--------------|----------------------|--------------------|---------------|-------------|
| sign(μ) | $\tan \beta$ | $M_{\chi_L^+}$ (GeV) | $ \lambda $ | $ \mu $ (GeV) | M_2 (GeV) |
| + | 1 | 200 | 0.72 | 290.8 | 271.2 |
| + | 5 | 200 | 1.40 | 125. | 125.8 |
| - | 1 | 200 | 0.72 | 290.8 | 186.8 |
| - | 5 | 200 | 1.40 | 125. | 151.3 |
| + | 1 | 400 | 0.72 | 290.8 | 340.8 |
| + | 5 | 400 | 1.40 | 125. | 379.6 |
| - | 1 | 400 | 0.72 | 290.8 | 390.6 |
| - | 5 | 400 | 1.40 | 125. | 383.9 |

Table 1: Numerical values of the input parameters and the corresponding derived fundamental parameters for $M_h = 125$ GeV and $M_{H^+} = 400$ GeV.

The corresponding decay widths for the radiative induced decays $h \rightarrow \gamma\gamma$ and $h \rightarrow Z\gamma$ of the lightest CP even Higgs boson h , in the framework of pure FP NMSSM model, are reported in Appendix.

In order to avoid a large tree-level Higgs decay into an invisible sector [46], that would destroy the potential enhancement of the Higgs decay into $\gamma\gamma$ [18], we will require that the mass of the lightest neutralino ($M_{\chi_L^0}$), which is the lightest supersymmetric state in our scenario, is heavier than half of the Higgs mass. Then, due to R -parity, all other Higgs decays into two generic neutralino states $h \rightarrow \chi_i^0 \chi_j^0$, including the case in which one or both are virtual states, will automatically vanish. In addition, we also require the lower bound on the chargino mass to be 90 GeV.

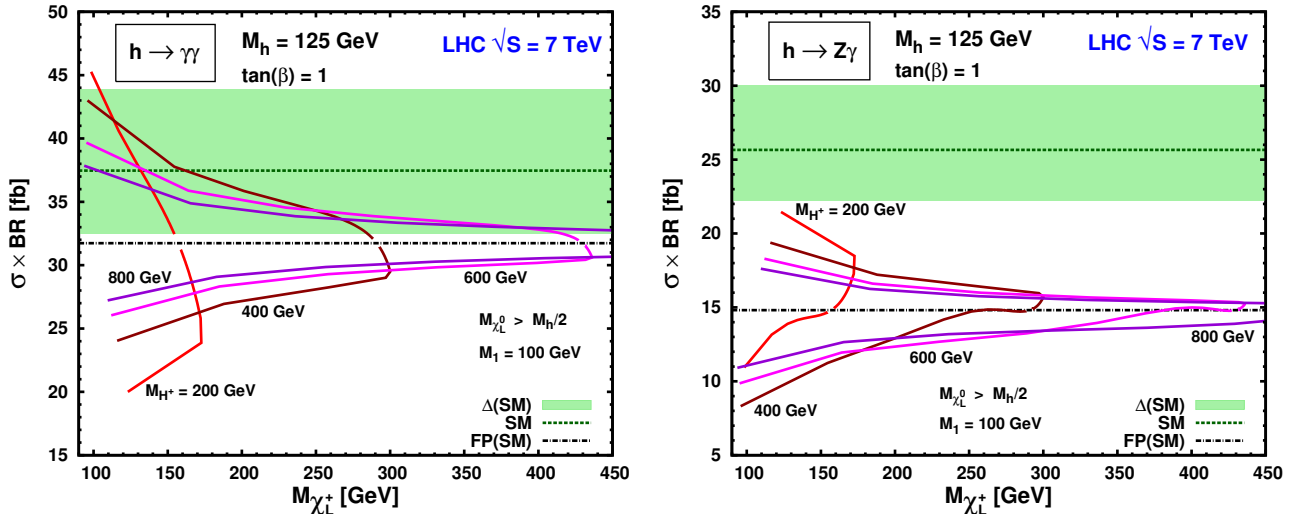


Figure 2: Radiatively induced signal rates of 125 GeV FP NMSSM Higgs decays $h \rightarrow \gamma\gamma$ (left) and $h \rightarrow Z\gamma$ (right) at the 7 TeV LHC as functions of the lightest chargino χ_L^+ mass ($M_{\chi_L^+}$) for several charged Higgs boson H^+ masses (M_{H^+}) as indicated in figures and for $\tan \beta = 1$. The SM central value prediction (dashed line) together with 1σ uncertainty band $\Delta(SM)$ and the FP SM Higgs prediction are also shown. The lines above (below) the FP SM line correspond to $\text{sign}(M_2\mu) > 0$ ($\text{sign}(M_2\mu) < 0$) for $h \rightarrow \gamma\gamma$ and to $\text{sign}(M_2\mu) < 0$ ($\text{sign}(M_2\mu) > 0$) for $h \rightarrow Z\gamma$.

Taking into account the results obtained so far, we have computed the $h \rightarrow \gamma\gamma$ and $h \rightarrow Z\gamma$ signal rates for the FP Higgs boson in the FP NMSSM. We present our results in Fig. 2 where we plot the signal rates of those processes as functions of the lightest chargino mass $M_{\chi_L^+}$ for different charged Higgs boson masses as indicated in the figure. The SM predictions together with their uncertainties and the FP SM predictions are also presented. The 1σ (green) band corresponds to the theoretical uncertainty on the SM production cross section by gluon-gluon fusion. We have not included the uncertainty band on the SM FP line since the corresponding theoretical uncertainty due to the VBF cross section is quite small and can be neglected in this context.

As in the MSSM case, the dominant contribution to SUSY contribution to $h \rightarrow \gamma\gamma$ and $h \rightarrow Z\gamma$ amplitudes comes from the charginos loop. From Figs. 2, 3, we can see that for fixed chargino mass there are always two solutions for the one-loop SUSY amplitudes corresponding to $h \rightarrow \gamma\gamma$ and $h \rightarrow Z\gamma$ decays. This can be understood as follows. For values of $M_{\chi_L^+}$ below the intersection point with the FP(SM) line, the double solution is mainly due to the sign of μ that controls the relative sign of the SUSY amplitude with respect to the SM one. The lines above (below) the FP SM line correspond to $\text{sign}(M_2\mu) > 0$ ($\text{sign}(M_2\mu) < 0$) for $h \rightarrow \gamma\gamma$ and to $\text{sign}(M_2\mu) < 0$ ($\text{sign}(M_2\mu) > 0$) for $h \rightarrow Z\gamma$. The dependence of the curves by $\text{sign}(M_2\mu)$ can be understood from Eqs.(66,67) in appendix.

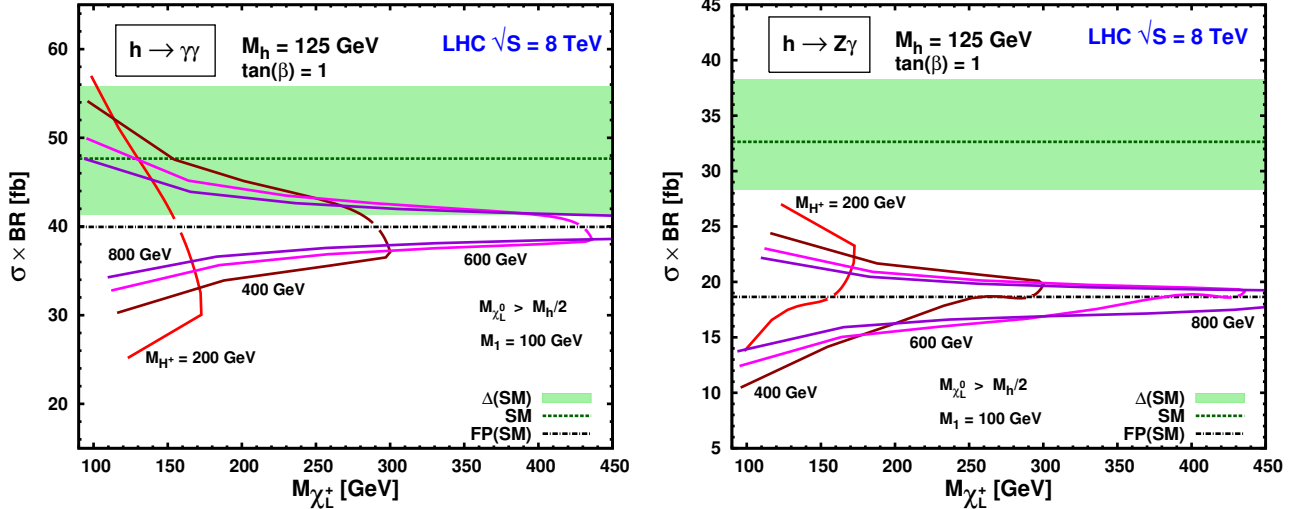


Figure 3: The same as in Fig. 2 but for a $M_h = 125$ GeV FP Higgs boson at the 8 TeV LHC.

However, for values of $M_{\chi_L^+}$ above the intersection point, the sign of μ is fixed and the double solution corresponds to the fact that in the loop run two non-degenerates values of heavy chargino states at fixed $M_{\chi_L^+}$. These two values of heavy chargino mass, for a fixed light chargino mass, correspond to the two different solutions for the M_2 parameter in eq. (64). The kink point corresponds to the case where the two solutions for the heavy chargino masses coincide. As we can see, there is a non-decoupling effect of the SUSY contribution to the loop $\gamma\gamma$ and $Z\gamma$ decay amplitudes in correspondance of the maximum value for the highest chargino mass.

As seen in the Figs. 2, 3, the FP NMSSM signal rates can be both bigger or smaller than the FP SM predictions. For very light sparticles the total rate in $\gamma\gamma$ channel can even exceed the SM prediction. On the other hand, the present fits indicate that the LHC observes fewer $\gamma\gamma$ events than predicted by the pure FP SM [18]. This result can be easily explained in the FP NMSSM since also rate reductions of as much as 50% are possible for the chosen parameters. The absence of points in the half-plane above (below) the FP(SM) line for the curve corresponding to $M_{H^+} = 200$ GeV in the case of $h \rightarrow \gamma\gamma$ ($h \rightarrow Z\gamma$), is due to the highest neutralino mass constraint $M_{\chi_L^0} > M_h/2$ and depends on our choice for $M_1 = 100$ GeV.

At the 8 TeV LHC the predictions are qualitatively the same but numerically different. We present the rates for 8 TeV LHC in Fig. 3 for the same model parameters as in Fig. 2.

If the top Yukawa coupling of the Higgs boson is not exactly vanishing, also gluon-gluon fusion production process will contribute to the Higgs production. In that case it is important to know our predictions for the FP Higgs branching fractions in our scenario. In Fig. 4 we plot the deviation of FP NMSSM Higgs boson branching fractions from the SM prediction for the previously specified parameters. The qualitative behaviour of branching fractions is the same as in previous figures, explaining our results.

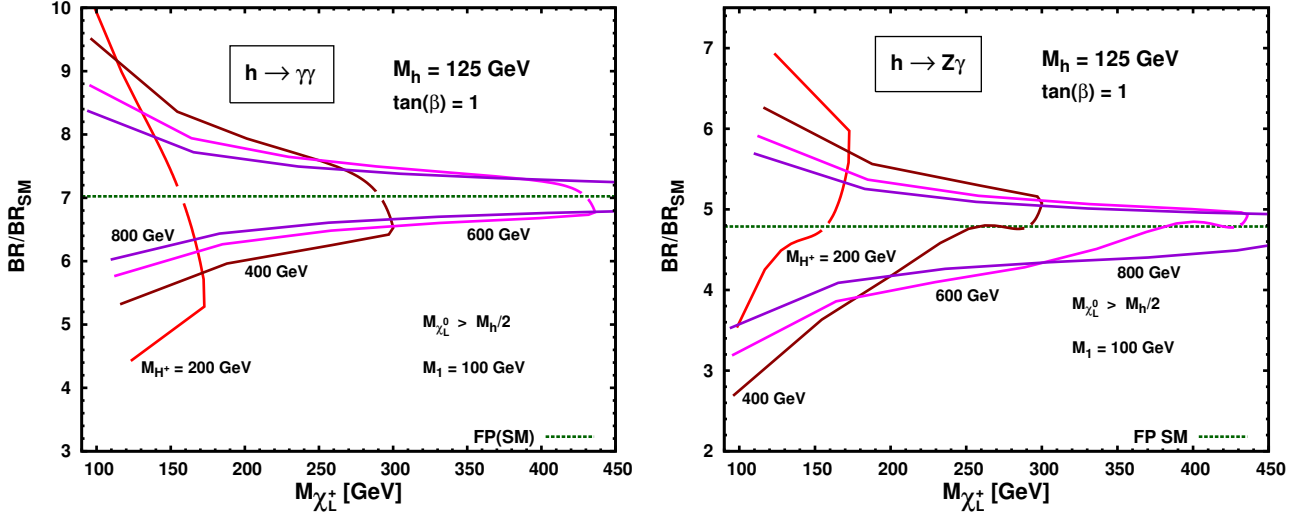


Figure 4: Dependence of the FP NMSSM Higgs boson branching fraction over the SM value as a function of the lightest chargino mass $M_{\chi_L^+}$ for $M_h = 125$ GeV, for different values of the charged Higgs boson mass M_H^+ and for $\tan \beta = 1$. The dashed line corresponds to the FP SM scenario. The lines above (below) the FP SM line correspond to $\text{sign}(M_2 \mu) > 0$ ($\text{sign}(M_2 \mu) < 0$) for $h \rightarrow \gamma\gamma$ and to $\text{sign}(M_2 \mu) < 0$ ($\text{sign}(M_2 \mu) > 0$) for $h \rightarrow Z\gamma$.

Finally, in Figs. 5 and 6 we present the same plots as in Figs. 2 and 4, respectively, for $\tan \beta = 5$. We set this value as an intermediate point between $\tan \beta = 1$ and the λ -SUSY upper bound $\tan \beta < 8$ at $M_h = 125$ GeV (see Fig. 1). By increasing $\tan \beta$, the deviations from the SM FP Higgs predictions for production rates and BR's for $h \rightarrow \gamma\gamma$ and $h \rightarrow Z\gamma$ are quite decreased. The largest effect is indeed achieved for $\tan \beta = 1$. On the other hand, at $\tan \beta = 5$, the largest SUSY contribution is obtained for a charged Higgs mass $M_{H^+} \sim 400$ GeV and a light chargino mass $M_{\chi_L^+} < 150$ GeV. The curves corresponding to $M_{H^+} = 200$ are not present in Figs. 5 and 6, not being allowed for $\tan \beta = 5$, because of the constraint $M_{\chi_L^0} > M_h/2$.

4 Discussion

Apart from the Higgs boson phenomenology at the LHC discussed in the previous section, the FP NMSSM scenario has other important implications for SUSY phenomenology. As we have emphasized, the $b \rightarrow s\gamma$ and $B_s \rightarrow \mu\mu$ constraints on the charged Higgs mass are absent in this model. Thus the charged Higgs boson can be light and kinematically accessible at the LHC in the process $pp \rightarrow H^+ H^-$. The same may apply to other possible scalar and pseudo-scalar final states. While we have chosen to work with a particular model in which the Higgs boson is exactly SM-like, in general also other final states are possible, allowing to study the model parameters. However, because they are fermiophobic, their search strategy must be revised.

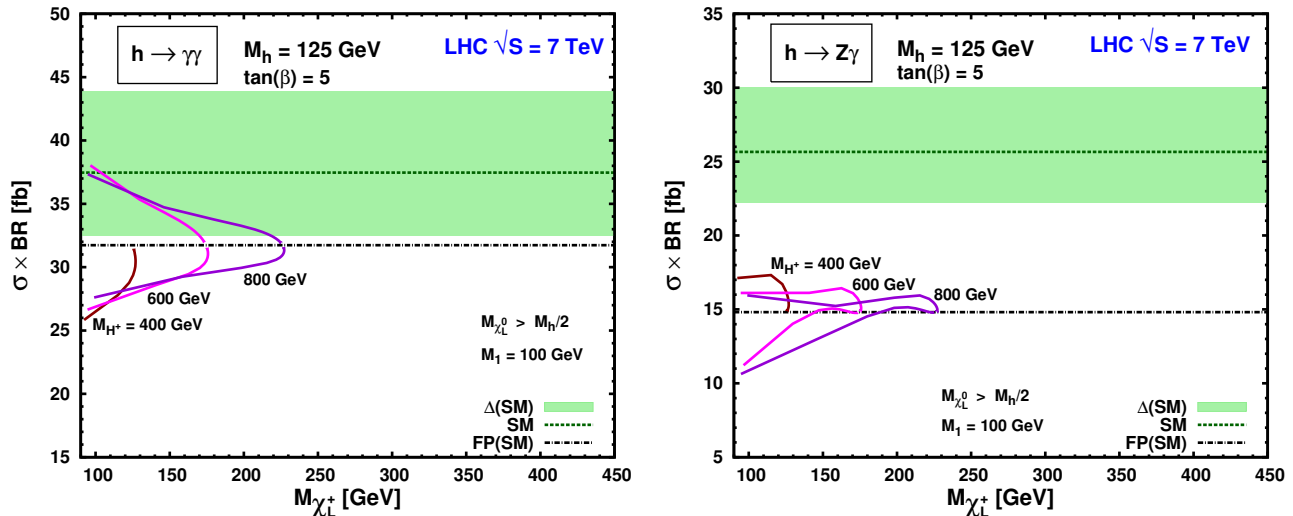


Figure 5: The same as in Fig. 2, but for $\tan \beta = 5$.

If neutralinos and charginos χ_i are light, the dominant decay modes of all heavy Higgs bosons H_i could be into two χ_i . In particular, the tree level decays of s_R are induced by the λ coupling. If the decay channels to sparticles are kinematically forbidden, the heaviest among A_1^0, A_2^0, H, H^\pm will have tree level decays into the lighter ones and to (real or virtual) W 's or Z 's. Then the lightest of them, since it cannot decay into SM fermions because of fermiophobia, will have SUSY induced radiative decays giving in the final state the SM gauge bosons and fermions. We stress that, because of the decoupling induced by our values of α and β , there are no trilinear vertices involving only one h and one of the scalars among A_1^0, A_2^0, H, H^\pm . Thus all the decays of heavier Higgs bosons are characterized either by large invisible branching fraction or multi-particle final states. Those decay signatures can easily be missed in present LHC searches explaining the absence of another Higgs-like resonance at higher masses.

The second most relevant phenomenological implication of our framework concerns direct dark matter searches. In the MSSM the spin-independent dark matter scattering off nuclei is dominated by tree level Higgs boson exchange. In the FP Higgs case this process is suppressed. The dominant dark matter scattering process is through WW exchange at one loop level. This implies that the scattering cross section is suppressed by additional loop factor compared with the MSSM expectations. Scattering due to W -loops is too weak [37] to be observed in the present stage of XENON100 [47].

Arguably the biggest drawback of our scenario is the absence of explanation for the third generation fermion masses. However, models of composite Higgs boson that explain naturalness of the electroweak symmetry breaking with new strong dynamics at 2–3 TeV scale do predict non-standard Higgs boson coupling to fermions [38]. Fermiophobia may be a feature of this framework. Supersymmetrizing the theory will stabilize the radiatively generated Yukawa couplings against new physics at high scales. While in non-SUSY case one expects large radiative corrections to Yukawa couplings proportional to $\log(M_h/\Lambda)$, where Λ is the unknown scale

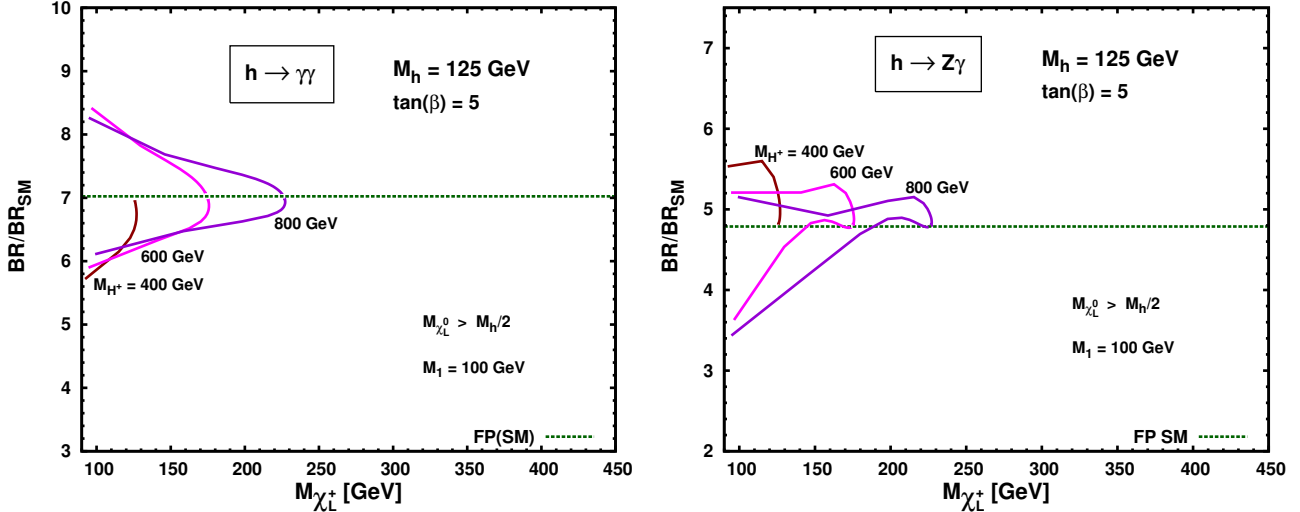


Figure 6: The same as in Fig. 4, but for $\tan \beta = 5$.

of new physics, in the SUSY version of FP Higgs those corrections will be at most of order $\log(M_h/M_{\text{SUSY}})$, hence stabilizing the theory.

5 Conclusions

If there is a signal of a fermiophobic, or partially fermiophobic, Higgs boson with mass $M_h = 125 \text{ GeV}$, the fundamental idea of supersymmetry, as it is implemented in the MSSM, is in trouble and must be revised. In particular, we have shown that the MSSM with vanishing or strongly suppressed Yukawa couplings is ruled out, independently of the particular supersymmetry breaking mechanism. Indeed, due to the absence of Yukawa couplings the usual (large) logarithmic corrections to the Higgs mass, induced by the scalar particles running in the loops, are absent and the upper bound on the Higgs mass is very close the M_Z mass.

In order to rescue supersymmetry, we show that a viable model beyond MSSM could be the NMSSM, where the absence of tree-level Yukawa couplings in the superpotential is guaranteed by the addition of a Z_3 discrete symmetry. The most relevant aspects of this scenario is that the SUSY naturalness criteria are automatically relaxed by a factor $N_c y_t^4/g^4 \sim 25$, solving the little hierarchy problem and allowing sparticle masses to be naturally of order 2–3 TeV. Moreover, the usual flavor and CP problems are relaxed partly because of the absence of Yukawa couplings and partly for the possibility that the scalar partners are naturally heavy.

In this framework, we consider the particular NMSSM case in which the mixing of the singlet with doublet Higgs fields is absent in the CP-even sector and at tree level the lightest Higgs boson is exactly SM-like. We analysed the predictions of this scenario for a $M_h = 125 \text{ GeV}$ Higgs at the LHC. We show that the predictions for the one-loop Higgs boson branching fractions and production rates in $\gamma\gamma$ and $Z\gamma$ can be sizably modified with respect to the FP SM model,

allowing a better fit to present collider data. However, the tree-level Higgs decay channels into WW^* and ZZ^* remain unaffected if the mixing between the singlet and doublet Higgs fields is absent. Relaxing this last condition, and so adding a new free parameter, the Higgs coupling to weak gauge boson WW and ZZ can be modified, and a suppression of the rates for $h \rightarrow WW^*$ and $h \rightarrow ZZ^*$ with respect to the pure FP model expectations can be achieved.

Finally, we would like to stress that the FP NMSSM offers a new arena for SUSY phenomenology at the LHC. In particular, most of the previous analyses on SUSY particle searches should be revised in the light of the fact that the large top-Yukawa coupling is absent or strongly suppressed. In addition, the stringent constraints from Higgs mediated and other FCNC processes can be relaxed due to the absence or suppressed Yukawa couplings, allowing for a light charged Higgs boson phenomenology at the LHC. Moreover, the interplay between chiral and supersymmetry breaking suggests that if there is a new strong dynamics at the TeV scale, as for instance indicated by the large top-quark mass, this could also play a role in the supersymmetry breaking mechanism, opening the way to a new and exciting phenomenology at the LHC.

Appendix

Here we provide the analytical expressions for the one-loop radiative decays widths of $h \rightarrow \gamma\gamma$ and $h \rightarrow Z\gamma$, where h is the lightest CP even Higgs boson, in the framework of pure FP NMSSM model. Following the results of Refs.[26], [48] we get

$$\begin{aligned} \Gamma(h \rightarrow \gamma\gamma) &= \frac{\alpha^2 G_F M_h^3}{128\sqrt{2}\pi^3} \left| g_{hWW} A_1^\gamma(\tau_W) + \frac{M_W^2 \lambda_{hH^+H^-}}{2c_W^2 M_{H^+}^2} A_0^\gamma(\tau_{H^+}) \right. \\ &\quad \left. + \sum_{i=1,2} \frac{2M_W}{M_{\chi_i^+}} g_{h\chi_i^+ \chi_i^-} A_{1/2}^\gamma(\tau_{\chi_i^+}) \right|^2, \end{aligned} \quad (66)$$

$$\begin{aligned} \Gamma(h \rightarrow Z\gamma) &= \frac{\alpha G_F^2 M_W^2 M_h^3}{64\pi^4} \left(1 - \frac{M_Z^2}{M_h^2} \right)^3 \left| g_{hWW} A_1^Z(\tau_W^{-1}, \lambda_W) \right. \\ &\quad + \frac{M_W^2 v_{H^\pm} \lambda_{hH^+H^-}}{2c_W M_{H^+}^2} A_0^Z(\tau_{H^+}^{-1}, \lambda_{H^+}) \\ &\quad \left. + \sum_{i=1,2; m=L,R} \frac{2M_W}{M_{\chi_i^+}} g_{h\chi_i^+ \chi_i^-} g_{Z\chi_i^+ \chi_i^-}^m A_{1/2}^Z(\tau_{\chi_i^+}^{-1}, \lambda_{\chi_i^+}) \right|^2, \end{aligned} \quad (67)$$

where G_F is the Fermi constant, α the electromagnetic fine structure constant, and the normalized Higgs and Z couplings appearing above are given by [26]

$$\begin{aligned}
g_{hWW} &= \sin(\beta - \alpha), \\
g_{h\chi_i^+ \chi_i^-} &= \frac{1}{\sqrt{2}s_W} \left(-\sin \alpha V_{i1} U_{i2} + \cos \alpha V_{i2} U_{i1} \right), \\
g_{Z\chi_i^+ \chi_j^-}^L &= \frac{1}{c_W} \left(s_W^2 - \frac{1}{2} V_{i2}^2 - V_{i1}^2 \right), \\
g_{Z\chi_i^+ \chi_j^-}^R &= \frac{1}{c_W} \left(s_W^2 - \frac{1}{2} U_{i2}^2 - U_{i1}^2 \right), \\
v_H^\pm &= \frac{2c_W^2 - 1}{c_W},
\end{aligned} \tag{68}$$

where $c_W = \cos \theta_W$ and $s_W = \sin \theta_W$, with θ_W the Weinberg angle, $\lambda_{hH^+H^-}$ is given in eq. (56), U_{ij} and V_{ij} the matrix elements of the corresponding U, V matrices diagonalizing the chargino mass matrix \mathbf{X} in Eq.(62) as $U\mathbf{X}V^{-1}$, and M_{χ_i} the corresponding eigenvalues.

The other symbols appearing in the expressions of the widths in Eqs.(66) and (67) are defined as $\tau_i = M_h^2/(4M_i^2)$, $\lambda_i = 4M_i^2/M_Z^2$, with $i = W, H^+, \chi_i^+$, while the functions $A_{(1/2,0,1)}^\gamma(x)$, and $A_{(1/2,0,1)}^Z(x, y)$ are given by [26],[48]

- for $h \rightarrow \gamma\gamma$

$$\begin{aligned}
A_{1/2}^\gamma(x) &= 2[x + (x-1)F(x)]x^{-2}, \\
A_0^\gamma(x) &= -[x - F(x)]x^{-2}, \\
A_1^\gamma(x) &= -[2x^2 + 3x + 3(2x-1)F(x)]x^{-2},
\end{aligned} \tag{69}$$

- for $h \rightarrow Z\gamma$

$$\begin{aligned}
A_{1/2}^Z(x, y) &= I_1(x, y) - I_2(x, y), \\
A_0^Z(x, y) &= I_1(x, y), \\
A_1^Z(x, y) &= c_W \left(4 \left(3 - \frac{s_W^2}{c_W^2} \right) I_2(x, y) + \left[\left(1 + \frac{2}{x} \right) \frac{s_W^2}{c_W^2} - \left(5 + \frac{2}{x} \right) \right] I_1(x, y) \right),
\end{aligned} \tag{70}$$

where the functions $I_{1,2}(x, y)$ are given by

$$\begin{aligned}
I_1(x, y) &= \frac{xy}{2(x-y)} + \frac{x^2y^2}{2(x-y)^2} (F(x^{-1}) - F(y^{-1})) + \frac{x^2y}{(x-y)^2} (G(x^{-1}) - G(y^{-1})), \\
I_2(x, y) &= -\frac{xy}{2(x-y)} (F(x^{-1}) - F(y^{-1})),
\end{aligned} \tag{71}$$

with $F(x) = (\arcsin \sqrt{x})^2$ for $x \leq 1$, and $G(x) = \sqrt{\frac{1-x}{x}} \arcsin \sqrt{x}$ for $x \leq 1$. The electromagnetic coupling constant α , appearing in eqs. (66) and (67), is evaluated at the scale $q^2 = 0$, since the final state photons in the Higgs decays $H \rightarrow \gamma\gamma$ and $H \rightarrow Z\gamma$ are on shell.

Acknowledgements

We thank A. Strumia for discussions. E.G. would like to thank the PH-TH division of CERN for its kind hospitality during the preparation of this work. This work was supported by the ESF grants 8090, 8499, 8943, MTT8, MTT59, MTT60, MJD140, JD164, by the recurrent financing SF0690030s09 project and by the European Union through the European Regional Development Fund.

References

- [1] The TEVNPH Working Group, f. t. CDF and D0 Collaborations, arXiv:1203.3774 [hep-ex].
- [2] CDF Collaboration, CDF Note 10806. D0 Collaboration, D0 Note 6303. Talk at the Moriond 2012 EW session.
- [3] ATLAS Collaboration, arXiv:1202.1414 [hep-ex].
- [4] CMS Collaboration, arXiv:1202.1487 [hep-ex]. CMS Collaboration, CMS-PAS-HIG-12-001.
- [5] ATLAS Collaboration, arXiv:1202.1415 [hep-ex].
- [6] CMS Collaboration, CMS-PAS-HIG-11-025, 2011.
- [7] CMS Collaboration, arXiv:1202.1489 [hep-ex].
- [8] CMS Collaboration, CMS-PAS-HIG-11-024, ATLAS Collaboration, ATLAS-CONF-2012-012
- [9] CMS Collaboration, arXiv:1202.4083. CMS Collaboration, CMS-PAS-HIG-12-007. ATLAS Collaboration, ATLAS-CONF-2012-014.
- [10] CMS Collaboration, CMS-PAS-HIG-11-031. ATLAS Collaboration, ATLAS-CONF-2012-015.
- [11] ATLAS Collaboration, arXiv:1202.1408 [hep-ex].
- [12] CMS Collaboration, arXiv:1202.1488 [hep-ex].
- [13] F. Englert and R. Brout, Phys. Rev. Lett. **13**, 321 (1964). P. W. Higgs, Phys. Lett. **12** (1964) 132. P. W. Higgs, Phys. Rev. Lett. **13**, 508 (1964). G. S. Guralnik, C. R. Hagen and T. W. B. Kibble, Phys. Rev. Lett. **13**, 585 (1964).

- [14] D0 Collaboration talk, CDF Collaboration talk, and TeVatron combination talk at Moriond 2012. ATLAS Collaboration talk, CMS Collaboration talk at Moriond 2012. Searches for the BSM Higgs boson: TeVatron combination talk, ATLAS and CMS Collaboration talks at Moriond 2012. CMS-PAS-HIG-12-001. CMS-PAS-HIG-12-006. <http://indico.in2p3.fr/conferenceOtherViews.py?view=standard&confId=6001>
- [15] J. L. Basdevant, E. L. Berger, D. Dicus, C. Kao and S. Willenbrock, Phys. Lett. B 313, 402 (1993) [arXiv:hep-ph/9211225]. V. D. Barger, N. G. Deshpande, J. L. Hewett and T. G. Rizzo, [arXiv:hep-ph/9211244]. P. Bamert and Z. Kunszt, Phys. Lett. B 306, 335 (1993) [arXiv:hep-ph/9303239]. H. Pois, T. J. Weiler and T. C. Yuan, Phys. Rev. D 47, 3886 (1993) [arXiv:hep-ph/9303277]. A. Stange, W. J. Marciano and S. Willenbrock, Phys. Rev. D 49, 1354 (1994) [arXiv:hep-ph/9309294]. M. A. Diaz and T. J. Weiler, arXiv:hep-ph/9401259. A. G. Akeroyd, Phys. Lett. B 368, 89 (1996) [arXiv:hep-ph/9511347]. A. G. Akeroyd, Phys. Lett. B **368**, 89 (1996) [hep-ph/9511347]. A. G. Akeroyd, J. Phys. G G **24**, 1983 (1998) [hep-ph/9803324]. A. Barroso, L. Brucher and R. Santos, Phys. Rev. D **60** (1999) 035005 [hep-ph/9901293]. L. Brucher and R. Santos, Eur. Phys. J. C **12** (2000) 87 [hep-ph/9907434].
- [16] CMS Collaboration, CMS-PAS-HIG-12-002. CMS Collaboration, CMS-PAS-HIG-12-008. ATLAS Collaboration, ATLAS-CONF-2012-013.
- [17] E. Gabrielli, B. Mele and M. Raidal, arXiv:1202.1796 [hep-ph].
- [18] P. P. Giardino, K. Kannike, M. Raidal and A. Strumia, arXiv:1203.4254 [hep-ph].
- [19] D. Carmi, A. Falkowski, E. Kuflik and T. Volansky, arXiv:1202.3144. A. Azatov, R. Contino and J. Galloway, arXiv:1202.3415. J. R. Espinosa, C. Grojean, M. Muhlleitner and M. Trott, arXiv:1202.3697.
- [20] E. Gabrielli and B. Mele, Phys. Rev. D **82**, 113014 (2010) [Erratum-ibid. D **83**, 079901 (2011)] [arXiv:1005.2498 [hep-ph]]. E. Gabrielli and B. Mele, Phys. Rev. D **83**, 073009 (2011) [arXiv:1102.3361 [hep-ph]]. E. Gabrielli and B. Mele, arXiv:1112.5993 [hep-ph].
- [21] E. L. Berger, Z. Sullivan and H. Zhang, arXiv:1203.6645 [hep-ph].
- [22] For a review and references see, J. Elias-Miro, J. R. Espinosa, G. F. Giudice, G. Isidori, A. Riotto and A. Strumia, arXiv:1112.3022; Z. -z. Xing, H. Zhang and S. Zhou, arXiv:1112.3112.
- [23] M. Kadastik, K. Kannike, A. Racioppi and M. Raidal, arXiv:1112.3647. M. Gonderinger, H. Lim and M. J. Ramsey-Musolf, arXiv:1202.1316 [hep-ph]. J. Elias-Miro, J. R. Espinosa, G. F. Giudice, H. M. Lee and A. Strumia, arXiv:1203.0237 [hep-ph]. O. Lebedev, arXiv:1203.0156 [hep-ph]. C. -S. Chen and Y. Tang, arXiv:1202.5717 [hep-ph]. C. Cheung, M. Papucci and K. M. Zurek, arXiv:1203.5106 [hep-ph].
- [24] J. McDonald, Phys. Rev. D 50, 3637 (1994) [arXiv:hep-ph/0702143]. C. P. Burgess, M. Pospelov and T. ter Veldhuis, Nucl. Phys. B 619, 709 (2001) [arXiv:hep-ph/0011335].

- [25] R. Barbieri, L. J. Hall and V. S. Rychkov, Phys. Rev. D **74** (2006) 015007 [hep-ph/0603188].
- [26] For a review of the MSSM phenomenology see, A. Djouadi, Phys. Rept. **459** (2008) 1 [hep-ph/0503173].
- [27] For MSSM studies in the context of 125 GeV Higgs boson see, L. J. Hall, D. Pinner and J. T. Ruderman, arXiv:1112.2703. H. Baer, V. Barger and A. Mustafayev, arXiv:1112.3017. S. Heinemeyer, O. Stal and G. Weiglein, arXiv:1112.3026. A. Arbey, M. Battaglia, A. Djouadi, F. Mahmoudi and J. Quevillon, Phys. Lett. B 708 (2012) 162 [arXiv:1112.3028]. A. Arbey, M. Battaglia and F. Mahmoudi, Eur. Phys. J. C 72 (2012) 1906 [arXiv:1112.3032]. M. Carena, S. Gori, N. R. Shah and C. E. M. Wagner, arXiv:1112.3336. P. Draper, P. Meade, M. Reece and D. Shih, arXiv:1112.3068. M. Kadastik, K. Kannike, A. Racioppi and M. Raidal, arXiv:1112.3647. O. Buchmueller, R. Cavanaugh, A. De Roeck, M. J. Dolan, J. R. Ellis, H. Flacher, S. Heinemeyer and G. Isidori *et al.*, arXiv:1112.3564. J. Cao, Z. Heng, D. Li and J. M. Yang, arXiv:1112.4391. A. Arvanitaki and G. Villadoro, JHEP 1202 (2012) 144 [arXiv:1112.4835]. Z. Kang, J. Li and T. Li, arXiv:1201.5305. K. A. Olive, arXiv:1202.2324. J. Ellis and K. A. Olive, arXiv:1202.3262. H. Baer, V. Barger and A. Mustafayev, arXiv:1202.4038. N. Desai, B. Mukhopadhyaya and S. Niyogi, arXiv:1202.5190. J. Cao, Z. Heng, J. M. Yang, Y. Zhang and J. Zhu, arXiv:1202.5821. J. Cao, Z. Heng, J. M. Yang and J. Zhu, arXiv:1203.0694. F. Jegerlehner, arXiv:1203.0806. Z. Kang, T. Li, T. Liu, C. Tong and J. M. Yang, arXiv:1203.2336. D. Curtin, P. Jaiswal and P. Meade, arXiv:1203.2932. N. Christensen, T. Han and S. Su, arXiv:1203.3207.
- [28] For a review of the NMSSM phenomenology see, U. Ellwanger, C. Hugonie and A. M. Teixeira, Phys. Rept. **496** (2010) 1 [arXiv:0910.1785 [hep-ph]]. M. Maniatis, Int. J. Mod. Phys. A **25** (2010) 3505 [arXiv:0906.0777 [hep-ph]].
- [29] For NMSSM studies in the context of 125 GeV Higgs boson see, L. J. Hall, D. Pinner and J. T. Ruderman, arXiv:1112.2703 [hep-ph]. U. Ellwanger, arXiv:1112.3548. M. Gozdz, arXiv:1201.0875. J. F. Gunion, Y. Jiang and S. Kraml, arXiv:1201.0982. S. F. King, M. Muhlleitner and R. Nevzorov, arXiv:1201.2671. Z. Kang, J. Li and T. Li, arXiv:1201.5305. D. A. Vasquez, G. Belanger, C. Boehm, J. Da Silva, P. Richardson and C. Wymant, arXiv:1203.3446. U. Ellwanger and C. Hugonie, arXiv:1203.5048 [hep-ph].
- [30] R. Barbieri and A. Strumia, [hep-ph/0007265].
- [31] M. Kadastik, K. Kannike, A. Racioppi and M. Raidal, Phys. Rev. Lett. **104** (2010) 201301 [arXiv:0912.2729 [hep-ph]].
- [32] S. R. Coleman and E. J. Weinberg, Phys. Rev. D **7** (1973) 1888.
- [33] N. Arkani-Hamed and S. Dimopoulos, JHEP **0506** (2005) 073 [hep-th/0405159]. G. F. Giudice and A. Romanino, Nucl. Phys. B **699** (2004) 65 [Erratum-ibid. B **706** (2005) 65] [hep-ph/0406088].

- [34] CMS Collaboration, CMS-PAS-SUS-11-003, CMS-PAS-SUS-11-004, CMS-PAS-SUS-11-005, CMS-PAS-SUS-11-006, CMS-PAS-SUS-11-007, CMS-PAS-SUS-11-008, CMS-PAS-SUS-11-009, CMS-PAS-SUS-11-010, CMS-PAS-SUS-11-011, CMS-PAS-SUS-11-012, CMS-PAS-SUS-11-013, CMS-PAS-SUS-11-015, CMS-PAS-SUS-11-017, CMS-PAS-SUS-11-018, CMS-PAS-SUS-11-019, CMS-PAS-SUS-11-020, CMS-PAS-SUS-12-005.
- [35] ATLAS Collaboration, ATLAS-CONF-2011-086, ATLAS-CONF-2011-090, ATLAS-CONF-2011-098, ATLAS-CONF-2011-130, ATLAS-CONF-2011-155, ATLAS-CONF-2011-156, ATLAS-CONF-2012-001, ATLAS-CONF-2012-002, ATLAS-CONF-2012-005, ATLAS-CONF-2012-022, ATLAS-CONF-2012-023, ATLAS-CONF-2012-035, ATLAS-CONF-2012-036, ATLAS-CONF-2012-033, ATLAS-CONF-2012-034, ATLAS-CONF-2012-037, ATLAS-CONF-2012-041.
- [36] R. Aaij *et al.* [LHCb Collaboration], arXiv:1203.4493 [hep-ex]. CMS Collaboration, Summary plot at CMS Wiki.
- [37] J. Hisano, K. Ishiwata and N. Nagata, Phys. Lett. B **690** (2010) 311 [arXiv:1004.4090 [hep-ph]].
- [38] G. F. Giudice, C. Grojean, A. Pomarol and R. Rattazzi, JHEP 0706 (2007) 045 [arXiv:hep-ph/0703164]. R. Contino, C. Grojean, M. Moretti, F. Piccinini and R. Rattazzi, JHEP 1005, 089 (2010) [arXiv:1002.1011]. R. Grober and M. Muhlleitner, JHEP 1106, 020 (2011) [arXiv:1012.1562]. S. De Curtis, M. Redi and A. Tesi, arXiv:1110.1613.
- [39] M. S. Carena, J. R. Espinosa, M. Quiros and C. E. M. Wagner, Phys. Lett. B **355** (1995) 209 [hep-ph/9504316].
- [40] L. M. Krauss and F. Wilczek, Phys. Rev. Lett. **62** (1989) 1221. J. Preskill and L. M. Krauss, Nucl. Phys. B **341** (1990) 50.
- [41] L. E. Ibanez and G. G. Ross, Phys. Lett. B **260** (1991) 291. L. E. Ibanez and G. G. Ross, Nucl. Phys. B **368** (1992) 3. H. K. Dreiner, C. Luhn and M. Thormeier, Phys. Rev. D **73** (2006) 075007 [hep-ph/0512163].
- [42] M. Chemtob and P. N. Pandita, Phys. Rev. D **73** (2006) 055012 [hep-ph/0601159].
- [43] A. Vilenkin, Phys. Rept. **121** (1985) 263.
- [44] S. A. Abel, Nucl. Phys. B **480** (1996) 55 [hep-ph/9609323]. C. F. Kolda, S. Pokorski and N. Polonsky, Phys. Rev. Lett. **80** (1998) 5263 [hep-ph/9803310]. C. Panagiotakopoulos and K. Tamvakis, Phys. Lett. B **446** (1999) 224 [hep-ph/9809475].
- [45] R. Barbieri, L. J. Hall, Y. Nomura and V. S. Rychkov, Phys. Rev. D **75** (2007) 035007 [hep-ph/0607332].
- [46] M. Raidal and A. Strumia, Phys. Rev. D 84 (2011) 077701 [arXiv:1108.4903]. Y. Mambrini, Phys. Rev. D 84 (2011) 115017 [arXiv:1108.0671]. J. F. Kamenik and C. Smith, arXiv:1201.4814 [hep-ph]. A. Arhrib, R. Benbrik and N. Gaur, arXiv:1201.2644 [hep-ph].

X. -G. He, B. Ren and J. Tandean, arXiv:1112.6364 [hep-ph]. C. Cheung and Y. Nomura, arXiv:1112.3043 [hep-ph]. X. Chu, T. Hambye and M. H. G. Tytgat, 1112.0493 [hep-ph]. O. Lebedev, H. M. Lee and Y. Mambrini, Phys. Lett. B **707** (2012) 570 [arXiv:1111.4482 [hep-ph]]. C. Englert, J. Jaeckel, E. Re and M. Spannowsky, Phys. Rev. D **85** (2012) 035008 [arXiv:1111.1719 [hep-ph]]. I. Low, P. Schwaller, G. Shaughnessy and C. E. M. Wagner, Phys. Rev. D **85** (2012) 015009 [arXiv:1110.4405 [hep-ph]]. M. Pospelov and A. Ritz, Phys. Rev. D **84** (2011) 113001 [arXiv:1109.4872 [hep-ph]]. T. Cohen, J. Kearney, A. Pierce and D. Tucker-Smith, arXiv:1109.2604 [hep-ph]. X. -G. He and J. Tandean, Phys. Rev. D **84** (2011) 075018 [arXiv:1109.1277 [hep-ph]]. Y. Mambrini, Phys. Rev. D **84** (2011) 115017 [arXiv:1108.0671 [hep-ph]]. C. -S. Chen and Y. Tang, arXiv:1202.5717 [hep-ph]. V. Barger, M. Ishida and W. -Y. Keung, arXiv:1203.3456. J. Cao, Z. Heng, J. M. Yang and J. Zhu, arXiv:1203.0694 [hep-ph]. A. Djouadi, O. Lebedev, Y. Mambrini and J. Quevillon, Phys. Lett. B **709** (2012) 65 [arXiv:1112.3299]. V. Barger, M. Ishida and W. -Y. Keung, arXiv:1203.3456 [hep-ph].

- [47] E. Aprile *et al.* [XENON100 Collaboration], Phys. Rev. Lett. **107** (2011) 131302 [arXiv:1104.2549 [astro-ph.CO]].
- [48] A. Djouadi, Phys. Rept. **457**, 1 (2008) [hep-ph/0503172].